Multiaxial Deformation of Polymers: Strain Energy Density Function and Time Dependence

Yves Termonia

Central Research and Development, Experimental Station, E. I. du Pont de Nemours, Inc., Wilmington, Delaware 19880-0356

Received March 9, 1992; Revised Manuscript Received June 15, 1992

ABSTRACT: We have extended our previous work to the study of the time dependence of the stress–strain behavior of rubberlike polymers. That dependence is conveniently described with the help of the so-called strain energy density function, W. The knowledge of W is crucial for the determination of the state of stress at any given point in a deformed body. Our model results indicate that the partial derivatives of W with respect to the strain invariants, I_1 and I_2, are strongly dependent on time. We show that their sum, however, should be a constant as a consequence of the Valanis–Landel hypothesis. We also prove that a finite value of $\partial W/\partial I_2$ is the fingerprint of a nonaffine type of deformation. On the basis on our model results, a new expression is proposed for the dependence of W on the strain invariants.

1. Introduction

In a recent publication,[1] we reported on a molecular model for describing the response of a rubbery polymer network to multiaxial deformation. The model allows one to study in detail the interplay of cross-links and entanglements in controlling the deformation behavior. It also explicitly takes into account the roles of cross-link functionality, molecular weight and its distribution, chain slippage through entanglements, and chain fracture at maximum elongation. The combination of those molecular details with continuum-mechanical considerations is the key to the calculability of the strain energy density function. Several alternative molecular models have been proposed in the literature. These models can be grouped in four categories: constrained fluctuation,[2] primitive path,[3,4] sliplink,[5,6] and tube[7,8] models. The relative merits of these various approaches in fitting experimental data have been reviewed by Gottlieb and Gaylord.[9] Our model,[1] however, was found to better describe the peculiar and complex behavior of the strain energy derivatives observed experimentally at very small deformations and at high strains.

Our original model of ref 1 did not allow for any time dependence of the stress–strain curves. Chains were allowed to slip through entanglements when the difference in force in the two strands of a chain separated by an entanglement fell below an entanglement friction force. That simplification is removed in the present work and the time dependence of chain slippage and breakage is now fully described with the help of the theory of thermally activated rate processes.[10] The model results lead to a better understanding of the role of entanglements and the complex strain dependence of the energy density function, W. They, in turn, allow us to analytically derive an exact relationship between the partial derivatives of W with respect to the strain invariants I_1 and I_2. A semiempirical expression for W, which actually describes our data at small strains, is also proposed.

2. Model

The model has been described at length in ref 1. Here, we shall restrict ourselves to restating the basic features that are of interest for the present work.

2.1. Network Model and Chain Slippage. In our approach, the rubberlike polymer is modeled by an array of bonds on a lattice of nodes. Bonds represent chain strands whereas nodes denote entanglements and/or cross-links. The approach explicitly takes into account the density of entanglements, the functionality of the cross-links, the degree of completion of the cross-linking reaction, and the initial molecular weight and its distribution. The network is deformed on the computer and, for each value of the external strain, the positions of the entanglements and cross-links are recalculated by minimizing the net residual force acting on each lattice node. That process leads, for an imperfectly cross-linked network, to a nonaffine deformation with a continual redistribution of stress among the various chain strands. In the original work of ref 1, chains were then allowed to slip through entanglements when the difference in stress in the two strands of a chain (i) separated by an entanglement, $\Delta\sigma_i$, fell below an entanglement friction force f_e. In the present work, that process is made time dependent and chain slippage is performed with the help of a thermally activated process, i.e., at a rate[10]

$$\nu_i = \tau \exp[-(U - \beta\Delta\sigma_i)/kT] \tag{1}$$

in which τ is a thermal vibration frequency, whereas U and β are, respectively, an activation energy and volume. Following previous work,[11] we assume that the average length of a chain strand capable of a coordinated movement, at a rate given by eq 1, is of the order of a statistical segment length. The simulation of the chain slippage events is performed with the help of a Monte-Carlo lottery, which assigns to each strand a probability for slippage[11]

$$p_i = \nu_i/\nu_{max} \tag{2}$$

where ν_{max} is the highest rate of slippage among all chains (i). At the end of each slippage event, the time t is incremented by $1/[\nu_{max}n(t)]$, in which $n(t)$ denotes the total number of entanglements at time t. This slippage process leads to local changes in the number of statistical segments among strain strands and, occasionally, to chain disentanglement. Although chain breakage does not occur in the present simulations, which are done at small strains, the process can be modeled by using a similar technique.[11]

2.2. Force on a Chain Strand. In our approach, the force on a chain strand is calculated as follows. Let r and $w(r)$ denote the end-to-end vector length and the free energy of deformation for a given chain strand between two nodes (entanglements and/or cross-links). The engineering stresses σ_x and σ_y along the x and y directions for that strand are obtained from[1,12]

0024-9297/92/2225-5008$03.00/0 © 1992 American Chemical Society

$$\sigma_x = \partial w(r)/\partial\lambda_x = [dw(r)/dr][\partial r/\partial\lambda_x]$$

$$\sigma_y = \partial w(r)/\partial\lambda_y = [dw(r)dr][\partial r/\partial\lambda_y] \quad (3)$$

in which λ_x and λ_y are the draw ratios along the x- and y-directions, respectively. Equation 3 can be rewritten in simpler form

$$\sigma_x = f(r)[\partial r/\partial\lambda_x] \qquad \sigma_y = f(r)[\partial r/\partial\lambda_y] \quad (4)$$

in which

$$f(r) = dw(r)/dr \quad (5)$$

is the force along the end-to-end vector of the chain strand. The latter is obtained from

$$f(r) = (kT/l)\mathcal{L}^{-1}(r/nl) \quad (6)$$

In eq 6, $\mathcal{L}^{-1}$ represents the inverse Langevin function, whereas n and l denote respectively the number and length of the statistical segments for the strand.

Prior to deformation, the orientation angle θ of a chain strand with respect to any axis has an average value $\langle\cos^2\theta\rangle = 1/3$. For simplicity, we start in our approach with a regular lattice of nodes; i.e., all θ's have the same value and each strand lies along the diagonal of a cube of side r_0. Thus, upon *local* deformation by draw ratios λ_x and λ_y, the end-to-end vector length of the strand is given by

$$r = r_0[\lambda_x^2 + \lambda_y^2 + 1/(\lambda_x\lambda_y)^2]^{1/2} \quad (7)$$

in which we have assumed that the condition of incompressibility for the bulk material is also fulfilled at the level of every single strand, i.e. $\lambda_x\lambda_y\lambda_z = 1$. From eq 7, it follows that

$$\partial r/\partial\lambda_x = (r_0^2/r)[\lambda_x^2 - (\lambda_y\lambda_x)^{-2}]/\lambda_x$$

$$\partial r/\partial\lambda_y = (r_0^2/r)[\lambda_y^2 - (\lambda_y\lambda_x)^{-2}]/\lambda_y \quad (8)$$

Introducing eqs 8 into eqs 4 leads to

$$\sigma_x = f(r)(r_0^2/r)[\lambda_x^2 - (\lambda_y\lambda_x)^{-2}]/\lambda_x$$

$$\sigma_y = f(r)(r_0^2/r)[\lambda_y^2 - (\lambda_y\lambda_x)^{-2}]/\lambda_y \quad (9)$$

2.3. Strain Energy Density and Its Partial Derivatives. Equations 9 refer to the state of stress of a given chain strand. In practice, only average values for the whole network of N chains (per unit volume) can be measured. Henceforth, we shall use bold type to refer to the average stresses

$$\boldsymbol{\sigma}_x = \int \sigma_x \, dN$$

$$\boldsymbol{\sigma}_y = \int \sigma_y \, dN \quad (10)$$

and to the macroscopic draw ratios λ_x and λ_y. From continuum-mechanical considerations, the average stresses $\boldsymbol{\sigma}$ are related to the partial derivatives of the strain energy density function W for the network

$$\boldsymbol{\sigma}_x = 2\left(\lambda_x - \frac{1}{\lambda_x^3\lambda_y^2}\right)\left[\frac{\partial W(I_1,I_2)}{\partial I_1} + \lambda_y^2\frac{\partial W(I_1,I_2)}{\partial I_2}\right]$$

$$\boldsymbol{\sigma}_y = 2\left(\lambda_y - \frac{1}{\lambda_y^3\lambda_x^2}\right)\left[\frac{\partial W(I_1,I_2)}{\partial I_1} + \lambda_x^2\frac{\partial W(I_1,I_2)}{\partial I_2}\right] \quad (11)$$

in which the strain invariants I_1 and I_2 for an incompressible material are obtained from

$$I_1 = \lambda_x^2 + \lambda_y^2 + (\lambda_x\lambda_y)^{-2}$$

$$I_2 = (\lambda_x\lambda_y)^2 + \lambda_x^{-2} + \lambda_y^{-2} \quad (12)$$

The engineering stresses σ_x and σ_y can be easily measured for any biaxial deformation. Their knowledge together with eqs 11 can then be used to calculate the partial derivatives of W

$$\frac{\partial W(I_1,I_2)}{\partial I_1} = \frac{1}{2(\lambda_y^2 - \lambda_x^2)}\left[\frac{\lambda_y^3\sigma_y}{\lambda_y^2 - (\lambda_y\lambda_x)^{-2}} - \frac{\lambda_x^3\sigma_x}{\lambda_x^2 - (\lambda_y\lambda_x)^{-2}}\right]$$

$$\frac{\partial W(I_1,I_2)}{\partial I_2} = \frac{1}{2(\lambda_x^2 - \lambda_y^2)}\left[\frac{\lambda_y\sigma_y}{\lambda_y^2 - (\lambda_y\lambda_x)^{-2}} - \frac{\lambda_x\sigma_x}{\lambda_x^2 - (\lambda_y\lambda_x)^{-2}}\right] \quad (13)$$

3. Results and Discussion

The results to be presented are for rubber polymer networks similar to those studied in ref 1. Thus, the chains have an initial molecular weight equal to four times that between entanglements, M_e. For the latter, we take M_e = 8100 g/mol, which is set to correspond to $n = 22$ statistical segments.[13] These parameter values approximate those found for commercial poly(dimethylsiloxane) (PDMS) networks. The chains are cross-linked at their ends with tetrafunctional monomers and the degree of completeness of the chemical reaction is set equal to 98%. In eq 1, we take for simplicity $\tau = 1$, $U = 0$, and $\beta = 5$. The actual values for those parameters are immaterial for the present purpose, since we are only qualitatively interested in the time dependence of the stress–strain curves.

3.1. Time Dependence of $\partial W/\partial I_1$ and $\partial W/\partial I_2$. Figure 1a shows the time dependence (in arbitrary units) of the partial derivatives $\partial W/\partial I_1$ and $\partial W/\partial I_2$ *at small strains*. The results are for a general biaxial deformation with I_1 = 3.050 and I_2 = 3.047, which correspond to $\lambda_x = 0.96$ and $\lambda_y = 1.13$. The starting network is made of 56 cross-links and 366 entanglements, 89 of which are not trapped between entanglements. Figure 1b shows the decrease with time of the number of untrapped entanglements due to chain slippage. Inspection of Figure 1a reveals that $\partial W/\partial I_1$ and $\partial W/\partial I_2$ exhibit wide variations at short times. At large times, however, both quantities show two well-defined and opposite trends: $\partial W/\partial I_1$ decreases whereas $\partial W/\partial I_2$ increases. As the number of untrapped entanglements decreases toward zero (see Figure 1b), the derivatives tend toward two limiting values. Also represented in Figure 1a are the limits $\partial W/\partial I_1 = -0.187$ and $\partial W/\partial I_2 = 0.325$ (heavy bars on the rhs of the figure). The latter were obtained from the original model of ref 1, taking an entanglement friction force $f_e = 0$ and starting from a network in which all the untrapped entanglements were removed (see also Figures 4 and 5 in that connection). Inspection of Figure 1a shows an excellent agreement between the two sets of limiting values. That agreement gives strong confidence in the validity of our various computer algorithms for describing the processes of chain slippage and chain disentanglement. It also indicates that the time dependence of the $\partial W/\partial I_i$'s is due to nontrapped entanglements, in support of previous work by Curro et al.[14,15]

3.2. Time and Strain Dependence of the Sum ($\partial W/\partial I_1 + \partial W/\partial I_2$). Inspection of Figure 1a reveals that, in

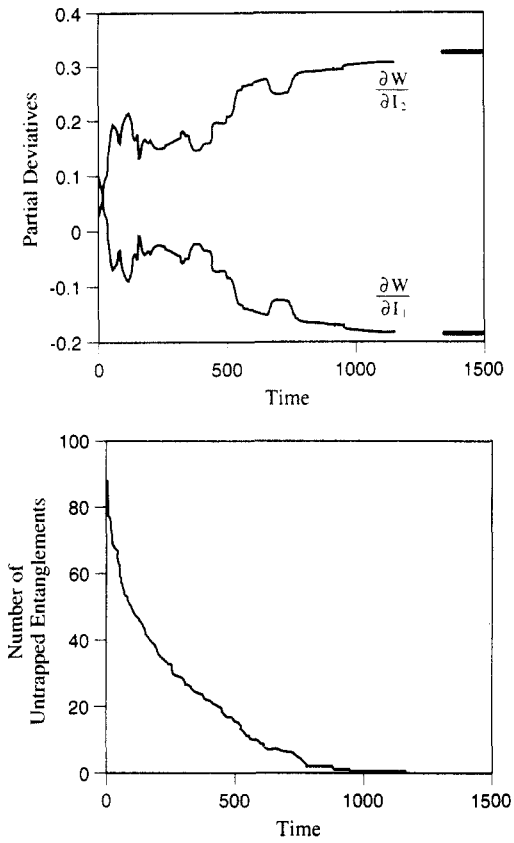

Figure 1. (a, Top) Time dependence (in arbitrary units) of the partial derivatives $\partial W/\partial I_1$ and $\partial W/\partial I_2$ at small strains. The results are for a general biaxial deformation with $I_1 = 3.050$ and $I_2 = 3.047$, which corresponds to $\lambda_x = 0.96$ and $\lambda_y = 1.13$. The heavy bars on the rhs denote the limiting values of $\partial W/\partial I_1$ and $\partial W/\partial I_2$ obtained from the original model of ref 1 with an entanglement friction force $f_e = 0$; see text. (b, Bottom) Time dependence of the number of entanglements that are not trapped between cross-links. The results are for the deformation described in Figure 1a.

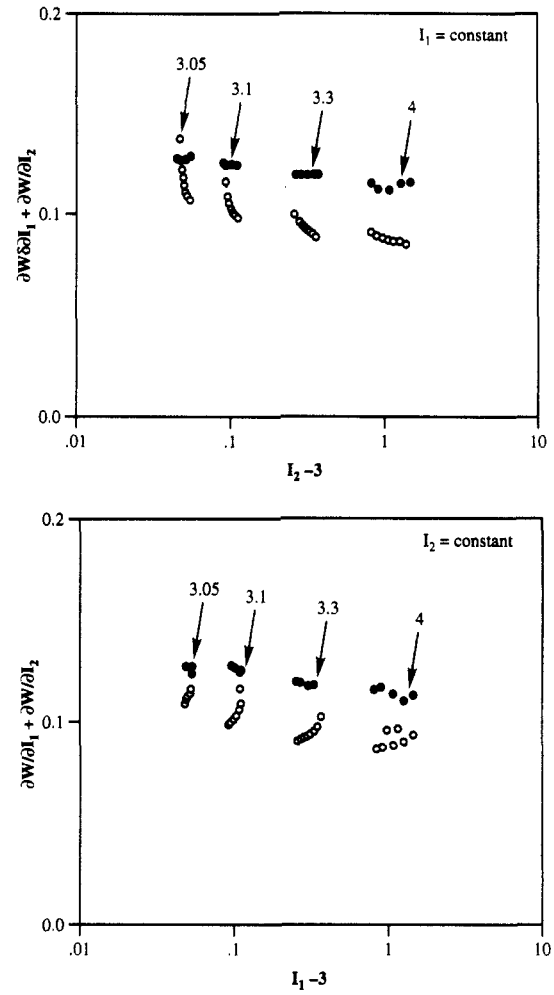

Figure 2. Strain dependence of the sum $(\partial W/\partial I_1 + \partial W/\partial I_2)$ at two different times. Open symbols (○) are for infinite times, taking an entanglement friction force $f_e = 0$; see Figure 1a in that connection. Filled-in symbols (●) are for a finite time, taking $f_e = 0.3$.[1]

spite of their strong dependence on time, $\partial W/\partial I_1$ and $\partial W/\partial I_2$ appear like mirror images of each other and the sum $(\partial W/\partial I_1 + \partial W/\partial I_2)$ remains nearly constant *with time*. It is interesting to note that previous experimental data[16,17] and simulation results from our model[1] also indicate a near-constancy of $(\partial W/\partial I_1 + \partial W/\partial I_2)$ *with strain*. The dependence of the sum $(\partial W/\partial I_1 + \partial W/\partial I_2)$ on time and strain is further studied in Figure 2. Open symbols (○) are for infinite times, taking an entanglement friction force $f_e = 0$; see Figure 1a in that connection. Filled-in symbols (●) are for finite times, taking $f_e = 0.3$.[1] The data clearly indicate that, despite the strong dependence of the partial derivatives on time and on draw ratios λ_x and λ_y, their sum shows a near-constancy with time and with strain.

We now turn to show analytically that the sum $(\partial W/\partial I_1 + \partial W/\partial I_2)$ should be a constant *at small strains and within the framework of the Valanis–Landel hypothesis*.[18] Omitting the arguments of W, eqs 11 can be rewritten in the form

$$\sigma_y - \sigma_x = 2(\lambda_y - \lambda_x)[\partial W/\partial I_1(1 + \lambda_x^{-3}\lambda_y^{-3}) + \partial W/\partial I_2(\lambda_x^{-3}\lambda_y^{-1} + \lambda_x^{-1}\lambda_y^{-3} + \lambda_x^{-2}\lambda_y^{-2} - \lambda_x\lambda_y)] \quad (14)$$

In the limit of small strains, λ_x and λ_y tend toward 1, and each of the two factors multiplying the derivatives inside the brackets approaches a value of 2. In that limit, eq 14 thus becomes

$$\sigma_y - \sigma_x \approx 4(\lambda_y - \lambda_x)[\partial W/\partial I_1 + \partial W/\partial I_2] \quad (15)$$

According to the Valanis–Landel hypothesis,[18] on the other hand, all the curves of $\sigma_y - \sigma_x$ vs λ_y at different λ_x values overlap by means of a vertical shift. That hypothesis, which has been verified on a number of vulcanized rubbers, therefore implies for eq 15

$$\partial W/\partial I_1 + \partial W/\partial I_2 \approx \text{constant} \quad (16)$$

Note that eqs 15 and 16 also predict (at small strains) a linear dependence of the curves $\sigma_y - \sigma_x$ on λ_y, in agreement with experimental observation[16,17] and previous results obtained with our model.[1]

3.3. Limit of Affine Deformation and $\partial W/\partial I_2 = 0$. As was stated in section 2.2, our model prior to deformation consists of a regular lattice of nodes (entanglements and cross-links) connected by chain strands having an equal number of statistical segments, $n = 22$. Upon deformation, slippage of chains through entanglements sets in, at a rate given by eq 1. This leads to local redistributions of the number of statistical segments among the various chain strands and eventually, see Figure 1b, to chain disentanglement. In the absence of chain slippage, however, entanglements act as cross-links and our lattice model retain its regularity at all times. The deformation then proceeds in a purely affine fashion, except for a few small regions due to an incompleteness of the cross-linking reaction ($p = 98\%$). Computer simulation results for the case of no chain slippage have been reported in ref 1 and, at small strains, they show $\partial W/\partial I_1 = \text{constant}$ and $\partial W/\partial I_2 = 0$. We now turn to prove those results analytically. In the case of affine deformation, $\lambda_i \equiv \lambda_i$ and $\sigma_i \equiv N\sigma_i$ ($i \equiv x$

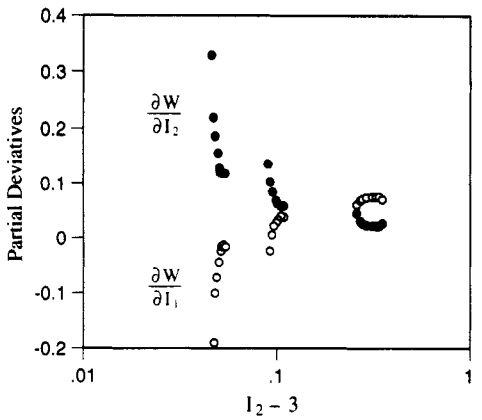

Figure 3. Strain dependence of the partial derivatives $\partial W/\partial I_1$ and $\partial W/\partial I_2$. The results were obtained after removing all entanglements that are not trapped between cross-links and not allowing any entanglement slippage thereafter.

or y) and substitution of eqs 9 and 10 into eqs 13 leads to

$$\frac{\partial W(I_1,I_2)}{\partial I_1} = \frac{Nf(r)(r_0^2/r)}{2} = (NkT)/2$$

$$\frac{\partial W(I_1,I_2)}{\partial I_2} = 0 \qquad (17)$$

In deriving the last equality in the first of eqs 17, we have used the fact that $r_0 = n^{1/2}l/3^{1/2}$ and taken the limit of small strains for which[19]

$$\mathcal{L}^{-1}(r/nl) = 3(r/nl) \qquad (18)$$

We show, in Appendix A, that eqs 17 also lead to the classical stress–strain relation for the limiting case of uniaxial extension.

To conclude, eqs 17 indicate that, for an affine deformation, $\partial W/\partial I_1$ is constant (at small strains), whereas $\partial W/\partial I_2$ is identically zero. In other words, entanglement slippage per se is not responsible for a nonzero $\partial W/\partial I_2$. Rather, it is the nonaffine type of deformation it brings about[13] that leads to a nonzero $\partial W/\partial I_2$. That important conclusion is further corroborated by the results of Figure 3. The figure is for networks in which all the entanglements that are not trapped between cross-links were removed *prior to deformation*. During deformation, however, no slippage of chains through the remaining entanglements was allowed. Still, the figure again shows a strong dependence of both $\partial W/\partial I_1$ and $\partial W/\partial I_2$ on strain, which can be attributed only to a nonaffine type of deformation.

3.4. Semiempirical Expression for W. The classical theory for *affine* deformation of rubber networks leads to a strain energy density function of the form[19]

$$W = C_1(I_1 - 3) \qquad (19)$$

Since experiments show that W is also a function of I_2, eq 19 was later modified to

$$W = C_1(I_1 - 3) + f(I_1,I_2) \qquad (20)$$

in which various expressions were proposed for the functional dependence of f on I_1 and I_2.[18,20–25] From our model simulation results of section 3.3, it appears that $f(I_1,I_2)$ originates from a nonaffine deformation, which ties very well with the premise that led to eq 19. At small

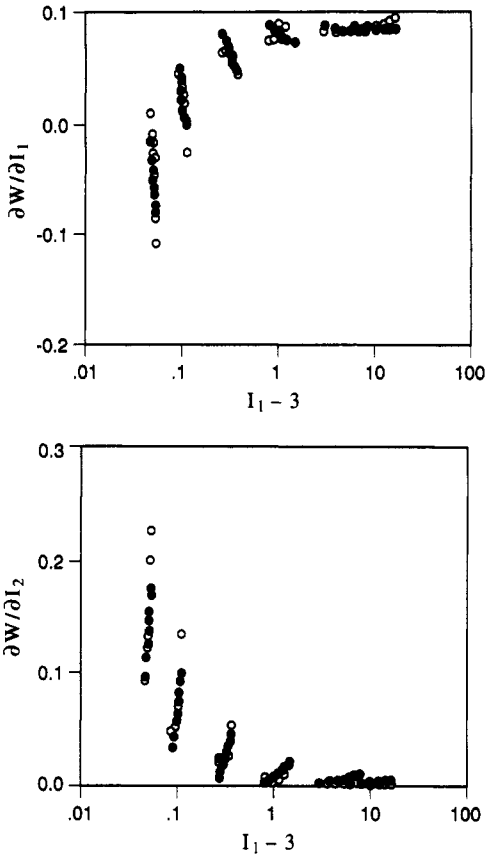

Figure 4. Strain dependence of the partial derivative $\partial W/\partial I_1$, as obtained from the present model (○) and from eqs 22 (●). Results for our model are for infinite times (see also Figures 1a and 2). Results from eqs 22 are for $C_1 = 0.0896$, $C_2 = 0.0032$, $C_{12} = -0.0021$, and $C_{21} = -0.0141$. (a, Top) Dependence on I_1 at different $I_2 = 3.05, 3.1, 3.3, 4, 7$, and 12. (b, Bottom) Dependence on I_2 at different $I_1 = 3.05, 3.1, 3.3, 4, 7$, and 12.

strains, the following expression for $f(I_1,I_2)$ is proposed

$$f(I_1,I_2) = C_2(I_2 - 3) + C_{12}(I_1 - 3)/(I_2 - 3) + C_{21}(I_2 - 3)/(I_1 - 3) \qquad (21)$$

Equations 20 and 21 lead to

$$\partial W/\partial I_1 = C_1 + C_{12}/(I_2 - 3) - C_{21}(I_2 - 3)/(I_1 - 3)^2$$

$$\partial W/\partial I_2 = C_2 - C_{12}(I_1 - 3)/(I_2 - 3)^2 + C_{21}(I_1 - 3) \qquad (22)$$

Note that eqs 22 resemble the relations proposed in ref 26 for the strain dependence of the $\partial W/\partial I_i$'s. Moreover, the sum

$$\partial W/\partial I_1 + \partial W/\partial I_2 = C_1 + C_2 + C_{12}(I_2 - I_1)/(I_2 - 3)^2 + C_{21}(I_1 - I_2)/(I_1 - 3)^2 \qquad (23)$$

satisfies eq 16 for the case $I_1 = I_2$. The performance of eqs 22 in fitting computer simulation data for the present model is studied in Figures 4 and 5. The simulation data (○) are for infinite times, which corresponds (see discussion of Figure 1a in that connection) to taking $f_e = 0$ in the original model of ref 1 and starting from a network in wich all the untrapped entanglements have been removed. The data fitted from eqs 22 (●) are for $C_1 = 0.0896$, $C_2 = 0.0032$, $C_{12} = -0.0021$, and $C_{21} = -0.0141$. Inspection of the figures shows a good agreement between the two sets of values at small strains, which, in turn, leads to confidence in the validity of our proposed eqs 20 and 21 for the dependence of the strain energy density function on I_1 and I_2.

Finally, as has been already noted in ref 1, our model predictions for the functional dependence of the partial

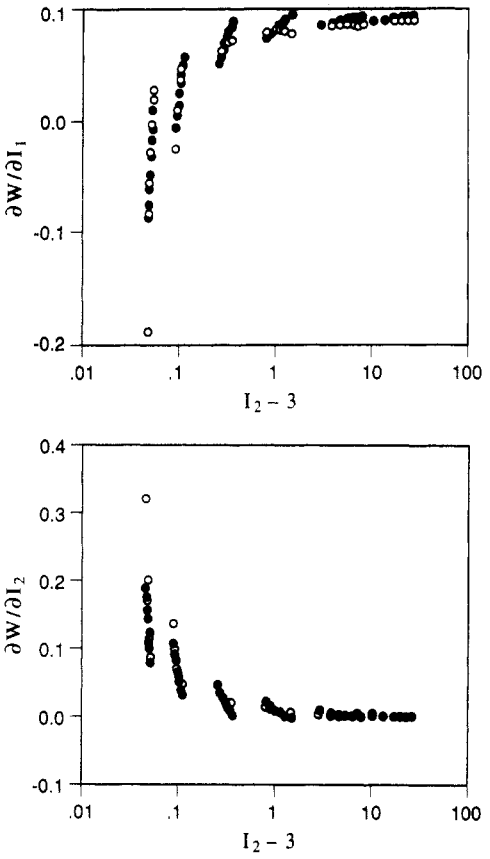

Figure 5. Same as Figure 4, but for $\partial W/\partial I_2$.

derivatives $\partial W/\partial I_i$ on strain agree in all respects with the experimental data of Becker.[16] They differ, however, from the data reported in ref 17. Our prediction of negative values for $\partial W/\partial I_1$ at small strains (Figure 4) has not been confirmed experimentally. We note, however, that the results of Figure 4 are for infinite times whereas experimental data are at 10-min relaxation[16,17] and they also clearly indicate a steady decrease of $\partial W/\partial I_1$ with time.[27]

4. Conclusions

We have extended the model of ref 1 to study the time dependence of the stress–strain behavior during biaxial deformation of rubberlike polymers. The following results are worth recapitulating:

(i) The partial derivatives $\partial W/\partial I_1$ and $\partial W/\partial I_2$ exhibit a strong dependence on time and their values at infinite times are identical with those of ref 1, taking an entanglement friction force, f_e, equal to zero.

(ii) Computer simulation results for the sum $(\partial W/\partial I_1 + \partial W/\partial I_2)$ show a near-constancy with time and with strain. We prove analytically that such an invariance can be derived from the Valanis–Landel hypothesis.

(iii) We show that a finite value of $\partial W/\partial I_2$ is the fingerprint of a nonaffine type of deformation.

(iv) We propose a new expression for the dependence of W on the strain invariants I_1 and I_2. The expression accurately reproduces the strong dependence of $\partial W/\partial I_1$ and $\partial W/\partial I_2$ on I_1 and I_2 at small strains.

Acknowledgment. I wish to thank Dr. D. J. Walsh for helpful discussions, which initiated the present research.

Appendix A

For the special case of simple uniaxial extension along the y-axis ($\sigma \equiv \sigma_y$, $\lambda \equiv \lambda_y = 1/\lambda_x^2$)[1]

$$\sigma = 2\left(\lambda - \frac{1}{\lambda^2}\right)\left[\frac{\partial W(I_1,I_2)}{\partial I_1} + \frac{1}{\lambda}\frac{\partial W(I_1,I_2)}{\partial I_2}\right] \quad \text{(A-1)}$$

and substitution of eqs 17 for an affine deformation in the limit of small strains leads to

$$\sigma = NkT\left(\lambda - \frac{1}{\lambda^2}\right) \quad \text{(A-2)}$$

in agreement with the classical result.[17]

References and Notes

(1) Termonia, Y. *Macromolecules* **1991**, *24*, 1128.
(2) Flory, P. J.; Erman, B. *Macromolecules* **1982**, *15*, 800.
(3) Graessley, W. W. *Adv. Polym. Sci.* **1982**, *46*, 67.
(4) Edwards, S. F. *Br. Polym. J.* **1977**, *9*, 140.
(5) Marrucci, G. *Rheol. Acta* **1979**, *18*, 193.
(6) Ball, R. C.; Doi, M.; Edwards, S. F.; Warner, M. *Polymer* **1981**, *22*, 1010.
(7) Marrucci, G. *Macromolecules* **1981**, *14*, 434.
(8) Gaylord, R. J. *Polym. Eng. Sci.* **1979**, *19*, 263.
(9) Gottlieb, M.; Gaylord, R. J. *Macromolecules* **1987**, *20*, 130.
(10) Kausch, H.-H. *Polymer Fracture*, 2nd ed.; Springer-Verlag: Berlin, 1987; p 73.
(11) Termonia, Y.; Smith, P. *Macromolecules* **1988**, *21*, 2184.
(12) Treloar, L. R. G.; Riding, G. *Proc. R. Soc. London* **1979**, *A369*, 261.
(13) Termonia, Y. *Macromolecules* **1989**, *22*, 3633.
(14) Curro, J. G.; Pearson, D. S.; Helfand, E. *Macromolecules* **1985**, *18*, 1157.
(15) Curro, J. G.; Pincus, P. *Macromolecules* **1983**, *16*, 559.
(16) Becker, G. W. *J. Polym. Sci., Part C* **1967**, *16*, 2893.
(17) Kawabata, S.; Matsuda, M.; Tei, K.; Kawai, H. *Macromolecules* **1981**, *14*, 154.
(18) Valanis, K. G.; Landel, R. F. *J. Appl. Phys.* **1967**, *38*, 2997
(19) Treloar, L. R. G. *The Physics of Rubber Elasticity*, 2nd ed.; Clarendon Press: Oxford, 1958.
(20) Mooney, M. *J. Appl. Phys.* **1940**, *11*, 582.
(21) Thomas, A. G. *Trans. Faraday Soc.* **1955**, *51*, 569.
(22) Gent, A. N.; Thomas, A. G. *J. Polym. Sci.* **1958**, *28*, 625.
(23) Hart-Smith, L. J. *J. Appl. Math. Phys.* **1966**, *17*, 608.
(24) Alexander, H. *Int. J. Eng. Sci.* **1968**, *6*, 549.
(25) Tschoegl, N. W. *J. Polym. Sci. A-1* **1970**, *9*, 1959.
(26) Obata, Y.; Kawabata, S.; Kawai, H. *J. Polym. Sci. A-2* **1970**, *8*, 903.
(27) Kawabata, S.; Kawai, H. *Adv. Polym. Sci.* **1977**, *24*, 89.